Effects of Neutron-Proton Short-Range Correlation on the Equation of State of Dense Neutron-Rich Nucleonic Matter

Bao-Jun Cai[1,2,3], Bao-An Li[1,a)] and Lie-Wen Chen[3]

[a)]Corresponding author and speaker: Bao-An.Li@tamuc.edu
[1]*Department of Physics and Astronomy, Texas A& M University-Commerce, Commerce, Texas, 75429, USA*
[2]*Department of Physics, Shanghai University, Shanghai 200444, China*
[3]*School of Physics and Astronomy and Shanghai Key Laboratory for Particle Physics and Cosmology, Shanghai Jiao Tong University, Shanghai 200240, China*

Abstract. The strongly isospin-dependent tensor force leads to short-range correlations (SRC) between neutron-proton (deuteron-like) pairs much stronger than those between proton-proton and neutron-neutron pairs. As a result of the short-range correlations, the single-nucleon momentum distribution develops a high-momentum tail above the Fermi surface. Because of the strongly isospin-dependent short-range correlations, in neutron-rich matter a higher fraction of protons will be depleted from its Fermi sea and populate above the Fermi surface compared to neutrons. This isospin- dependent nucleon momentum distribution may have effects on: (1) nucleon spectroscopic factors of rare isotopes, (2) the equation of state especially the density dependence of nuclear symmetry energy, (3) the coexistence of a proton-skin in momentum space and a neutron-skin in coordinate space (i.e., protons move much faster than neutrons near the surface of heavy nuclei). In this talk, we discuss these features and their possible experimental manifestations. As an example, SRC effects on the nuclear symmetry energy are discussed in detail using a modified Gogny-Hartree-Fock (GHF) energy density functional (EDF) encapsulating the SRC-induced high momentum tail (HMT) in the single-nucleon momentum distribution.

Single-nucleon momentum distribution function encapsulating SRC effects

It is well known that the SRC leads to a high (low) momentum tail (depletion) in the single-nucleon momentum distribution function denoted by $n_{\mathbf{k}}^J$ above (below) the nucleon Fermi surface in cold nucleonic matter [1, 2, 3, 4, 5]. Significant efforts have been made in recent years both theoretically and experimentally to constrain the isospin-dependent parameters characterizing the SRC-modified $n_{\mathbf{k}}^J$ in neutron-rich nucleonic matter. In particular, it has been found via analyzing electron-nucleus scattering data that the percentage of nucleons in the HMT above the Fermi surface is as high as about 28%±4% in symmetric nuclear matter (SNM) but decreases gradually to about only 1%∼2% in pure neutron matter (PNM). On the other hand, the predicted size of the HMT still depends on the model and interaction used. For instance, the self-consistent Green's function (SCGF) theory using the AV18 interaction predicts a 11%∼13% HMT for SNM at saturation density and a 4%∼5% HMT in PNM [6].

For completeness and the ease of the following discussions, we first briefly describe the SRC-modified single-nucleon momentum distribution function encapsulating a HMT constrained by the available SRC data that we shall use in this work. The single-nucleon momentum distribution function in cold asymmetric nuclear matter (ANM) has the following form [7, 8, 9, 10]

$$n_{\mathbf{k}}^J(\rho,\delta) = \begin{cases} \Delta_J, & 0 < |\mathbf{k}| < k_{\rm F}^J, \\ C_J\left(k_{\rm F}^J/|\mathbf{k}|\right)^4, & k_{\rm F}^J < |\mathbf{k}| < \phi_J k_{\rm F}^J. \end{cases} \tag{1}$$

Here, $k_{\rm F}^J = k_{\rm F}(1+\tau_3^J\delta)^{1/3}$ is the Fermi momentum where $k_{\rm F} = (3\pi^2\rho/2)^{1/3}$, $\tau_3^{\rm n} = +1$ and $\tau_3^{\rm p} = -1$, respectively, $\delta = (\rho_{\rm n}-\rho_{\rm p})/(\rho_{\rm n}+\rho_{\rm p})$ is the isospin asymmetry, and ϕ_J is a high-momentum cut-off parameter. The parameters

involved depend on the isospin asymmetry and satisfy the normalization condition [10]. The above form of $n^J_{\mathbf{k}}(\rho,\delta)$ was found consistent with the well-known predictions of microscopic nuclear many-body theories [1, 2, 3, 4] and the recent experimental findings [5]. This form of $n^J_{\mathbf{k}}(\rho,\delta)$ has been applied to address several issues regarding the HMT effects recently in both nuclear physics and astrophysics.

The parameters Δ_J, C_J and ϕ_J are assumed to depend linearly on δ based on predictions of microscopic many-body theories $Y_J = Y_0(1 + Y_1\tau_3^J\delta)$ [7]. The amplitude C_J and high-momentum cutoff coefficient ϕ_J determine the fraction of nucleons in the HMT via $x_J^{\rm HMT} = 3C_J\left(1-\phi_J^{-1}\right)$. Moreover, the normalization condition between the density ρ_J and the distribution $n^J_{\mathbf{k}}$, i.e., $[2/(2\pi)^3]\int_0^\infty n^J_{\mathbf{k}}(\rho,\delta)\mathrm{d}\mathbf{k} = \rho_J = (k_{\rm F}^J)^3/3\pi^2$ requires that only two of the three parameters, i.e., C_J, ϕ_J and Δ_J, are independent. Here we choose the first two as independent and determine the Δ_J by $\Delta_J = 1 - 3C_J(1-\phi_J^{-1}) = 1 - x_J^{\rm HMT}$. Meanwhile, the adopted $C/|\mathbf{k}|^4$ shape of the HMT both for SNM and PNM is strongly supported by recent studies both theoretically and experimentally. It is interesting to point out that the $|\mathbf{k}|^{-4}$ form of the HMT is also found in Bose system theoretically and experimentally, indicating a very general feature of the HMT. For comparisons, we use two HMT parameter sets. The $n^J_{\mathbf{k}}$ adopting a 28% HMT in SNM and a 1.5% HMT in PNM is abbreviated as the HMT-exp set, and that adopting a 12% HMT in SNM and a 4% HMT in PNM [6] as the HMT-SCGF set [10]. Moreover, the model using a step function for the $n^J_{\mathbf{k}}$ is denoted as the free Fermi gas (FFG) set as a reference. As discussed in more details in ref. [10], the HMT parameters in the HMT-exp (HMT-SCGF) parameter set are $\phi_0 \approx 2.38$ ($\phi_0 \approx 1.49$), $\phi_1 \approx -0.56$ ($\phi_1 \approx -0.25$), $C_0 \approx 0.161$ ($C_0 \approx 0.121$), and $C_1 \approx -0.25$ ($C_1 \approx -0.01$), respectively.

Incorporating SRC effects in Gogny Hartree-Fock energy density functionals

In most studies of heavy-ion collisions using transport models, one parameterizes the energy density functionals (EDFs) and determine their parameters by reproducing empirical properties of SNM at the saturation density ρ_0, a selected value of symmetry energy $E_{\rm sym}(\rho_0)$ and its slope $L \equiv [3\rho \mathrm{d}E_{\rm sym}(\rho)/\mathrm{d}\rho]_{\rho_0}$ as well as main features of nucleon optical potentials extracted from analyzing nucleon-nucleus scatterings, such as the isosclar and isovector nucleon effective masses and their asymptotic values at high momenta at ρ_0, etc., see, e.g., ref. [11] for detailed discussions. For example, using a modified Gogny-type momentum-dependent interaction (MDI) [12, 13, 14, 15, 16], a modified GHF-EDF in terms of the average energy per nucleon $E(\rho,\delta)$ in ANM at density ρ and isospin asymmetry δ can be written as

$$E(\rho,\delta) = \sum_{J=\mathrm{n,p}}\frac{1}{\rho_J}\int_0^\infty \frac{\mathbf{k}^2}{2M}n^J_{\mathbf{k}}(\rho,\delta)\mathrm{d}\mathbf{k} + \frac{A_\ell(\rho_{\rm p}^2+\rho_{\rm n}^2)}{2\rho\rho_0} + \frac{A_{\rm u}\rho_p\rho_n}{\rho\rho_0} + \frac{B}{\sigma+1}\left(\frac{\rho}{\rho_0}\right)^\sigma(1-x\delta^2)$$
$$+\sum_{J,J'}\frac{C_{J,J'}}{\rho\rho_0}\int \mathrm{d}\mathbf{k}\mathrm{d}\mathbf{k}' f_J(\mathbf{r},\mathbf{k})f_{J'}(\mathbf{r},\mathbf{k}')\Omega(\mathbf{k},\mathbf{k}'). \quad (2)$$

The first term is the kinetic energy while the second to fourth terms are the usual zero-range 2-body and effective 3-body contributions characterized by their strength parameters $A_\ell, A_{\rm u}$ and B as well as the density dependence σ of the 3-body force [14, 15]

$$A_\ell = A_\ell^0 + \frac{2xB}{1+\sigma},\ \ A_{\rm u} = A_{\rm u}^0 - \frac{2xB}{1+\sigma} \quad (3)$$

where x controls the competition between the isosinglet and isotriplet 2-body interactions, and it affects only the slope L but not the $E_{\rm sym}(\rho_0)$ by design [14]. The last term in Eq. (2) is the contribution to the Equation of State (EOS) from the finite-range 2-body interactions characterized by the strength parameter $C_{J,J} \equiv C_\ell$ for like and $C_{J,\overline{J}} \equiv C_{\rm u}$ for unlike nucleon paris, respectively, using the notations $\overline{\rm n}$ = p and $\overline{\rm p}$ = n. The $f_J(\mathbf{r},\mathbf{k})$ and $n^J_{\mathbf{k}}(\rho,\delta)$ are the nucleon phase space distribution function and momentum distribution function, respectively. In equilibrated nuclear matter at zero temperature, they are related by

$$f_J(\mathbf{r},\mathbf{k}) = \frac{2}{h^3}n^J_{\mathbf{k}}(\rho,\delta) = \frac{1}{4\pi^3}n^J_{\mathbf{k}}(\rho,\delta),\ \ \hbar = 1. \quad (4)$$

For example, in the FFG, $n^J_{\mathbf{k}} = \Theta(k_{\rm F}^J - |\mathbf{k}|)$ with Θ the standard step function, then $f_J(\mathbf{r},\mathbf{k}) = (1/4\pi^3)\Theta(k_{\rm F}^J - |\mathbf{k}|)$.

The regulating function $\Omega(\mathbf{k},\mathbf{k}')$ [13, 14] originating from the meson exchange theory of nuclear force normally has the form of

$$\Omega(\mathbf{k},\mathbf{k}') = \left[1+\left(\frac{\mathbf{k}-\mathbf{k}'}{\Lambda}\right)^2\right]^{-1} \tag{5}$$

where $\mathbf{k}$ and $\mathbf{k}'$ are the momenta of two interacting nucleons and Λ is a parameter regulating the momentum dependence of the single-particle potential. For applications to SNM, it is usually determined by fixing the nucleon isoscalar effective mass at the Fermi surface to an empirical value [13, 14]. In applying the above formalisms to transport model simulations of nuclear reactions, the $f_J(\mathbf{r},\mathbf{k})$ and $n^J_{\mathbf{k}}(\rho,\delta)$ are calculated self-consistently from solving dynamically the coupled Boltzmann-Uehling-Uhlenbeck (BUU) transport or molecular dynamics equations for quasi-nucleons [17, 18, 19]. While in studying thermal properties of hot nuclei or stellar matter in thermal equilibrium, the Fermi-Dirac distributions at finite temperatures are used.

Traditionally, one writes the EDF as a sum of kinetic EOS of FFG plus several potential terms. Before making any applications, the model parameters of the EDFs are normally fixed by using step functions for the $f_J(\mathbf{r},\mathbf{k})$ and $n^J_{\mathbf{k}}(\rho,\delta)$ as in a FFG at zero temperature in reproducing properties of nuclei or nuclear matter in their ground states. In reality, however, since all nucleons interact with each other in nuclear medium, they naturally become quasi-nucleons. The normal practice of optimizing the EDFs puts all effects of interactions into the potential part of the EDF thus ignores interaction effects on the kinetic energy of quasi-nucleons. The momentum distribution of these quasi-nucleons in the ground state of the system considered is not simply a step function if SRC effects are considered as we discussed in the previous section. Here, we separate the total EDF into a kinetic energy and several potential parts of quasi-nucleons. The $f_J(\mathbf{r},\mathbf{k})$ and $n^J_{\mathbf{k}}(\rho,\delta)$ with HMTs constrained by the SRC experiments are used in evaluating both the kinetic and the momentum-dependent potential parts of the EDF in ANM at zero temperature. At least for simulating heavy-ion collisions using transport models, how the total EDFs are separated into their kinetic and potential parts are important and have practical consequences in predicting experimental observables. Interestingly, how the SRC may affect the symmetry energy, heavy-ion reactions and properties of neutron stars are among the central issues in our pursuit of understanding the nature of neutron-rich nucleonic matter. Previous attempts to incorporate the experimentally constrained $n^J_{\mathbf{k}}(\rho,\delta)$ and $f_J(\mathbf{r},\mathbf{k})$ with HMT in the non-relativistic EDF and examine their effects on heavy-ion collisions and neutron stars were found very difficult. This is mainly because of the nontrivial momentum dependence of the $U_J(\rho,\delta,|\mathbf{k}|)$ and the EDF when the SRC-modified $n^J_{\mathbf{k}}(\rho,\delta)$ and $f_J(\mathbf{r},\mathbf{k})$ are used. Since one needs to solve 8-coupled equations simultaneously to obtain self-consistently all model parameters from inverting empirical properties of ANM and nucleon optical potentials at ρ_0, numerical problems associated with the momentum integrals in Eq. (2) using the original $\Omega(\mathbf{k},\mathbf{k}')$ are very difficult to solve.

A surrogate high-momentum regulating function for the MDI energy density functional

To overcome the numerical problem mentioned above, a surrogate high-momentum regulating function $\Omega(\mathbf{k},\mathbf{k}')$ that approximates very well the original one while enables all integrals in the EDF and $U_J(\rho,\delta,|\mathbf{k}|)$ to be analytically expressed was proposed recently in ref. [20]. Perturbatively, if Λ is large compared to the momenta scale in the problems under investigation, the $\Omega(\mathbf{k},\mathbf{k}')$ in Eq. (5) can be expanded as $\Omega(\mathbf{k},\mathbf{k}') \approx 1-\mathbf{k}^2/\Lambda^2-\mathbf{k}'^2/\Lambda^2+2\mathbf{k}\cdot\mathbf{k}'/\Lambda^2$. Using this as a hint, we parameterize the $\Omega(\mathbf{k},\mathbf{k}')$ as

$$\Omega(\mathbf{k},\mathbf{k}') = 1 + a\left[\left(\frac{\mathbf{k}\cdot\mathbf{k}'}{\Lambda^2}\right)^2\right]^{1/4} + b\left[\left(\frac{\mathbf{k}\cdot\mathbf{k}'}{\Lambda^2}\right)^2\right]^{1/6}, \tag{6}$$

where a and b are two new parameters. It is interesting to note that this $\Omega(\mathbf{k},\mathbf{k}')$ is invariant under the transformation $a \to a/\xi^{3/2}$, $b \to \xi b$ and $\Lambda \to \Lambda/\xi^{3/2}$, indicating that we have the freedom to first fix one of them without affecting the physical results. Here we set $b = 2$ and then determine the a and Λ using known constraints as we shall discuss in the following.

The advantages of using this new regulating function is twofold: firstly, the basically 1/2 and 1/3 power of $\frac{\mathbf{k}\cdot\mathbf{k}'}{\Lambda^2}$ in the second and third term in (6) is relevant for describing properly the energy dependence of nucleon optical potential [21]; secondly, it enables analytical expressions for the EOS and $U_J(\rho,\delta,|\mathbf{k}|)$ in ANM. We notice that the Ω function is only perturbatively effective at momenta smaller than the momentum scale Λ, indicating that the EDF

constructed can only be used to a restricted range of momentum/density. It turns out that the cut-off of the HMT in ANM up to about $3\rho_0$ is significantly smaller than the Λ parameter we use here. The above non-relativistic GHF-EDF is denoted as abMDI in the following.

TABLE 1. Coupling constants used in the three sets (right side) and some empirical properties of asymmetric nucleonic matter used to fix them (left side). $b = 2$ and $\Lambda = 1.6\,\mathrm{GeV/c}$ are used in this work. $K_0 \equiv K_0(\rho_0), M_0^* \equiv M_0^*(\rho_0), L \equiv L(\rho_0)$.

Quantity	Value	Coupling	FFG	HMT-SCGF	HMT-exp
ρ_0 (fm^{-3})	0.16	A_ℓ^0 (MeV)	−578.7397	614.1020	307.4366
$E_0(\rho_0)$ (MeV)	−16.0	A_u^0 (MeV)	225.6127	711.5675	1055.4219
M_0^*/M	0.58	B (MeV)	517.5297	−256.9850	−64.5669
K_0 (MeV)	230.0	C_ℓ (MeV)	−155.6406	−154.2604	−129.5643
$U_0(\rho_0, 0)$ (MeV)	−100.0	C_u (MeV)	−285.3256	−351.5893	−587.2980
$E_\mathrm{sym}(\rho_0)$ (MeV)	31.6	σ	1.0353	0.9273	0.6694
L (MeV)	58.9	a	−5.4511	−5.0144	−4.1835
$U_\mathrm{sym}(\rho_0, 1\,\mathrm{GeV})$ (MeV)	−20.0	x	0.6144	0.3703	0.1123

We fix all parameters in the model EDF using empirical properties of SNM, ANM and main features of nucleon optical potentials at ρ_0. More specifically, for SNM we adopt $E_0(\rho_0) = -16\,\mathrm{MeV}$ at the saturation density $\rho_0 = 0.16\,\mathrm{fm}^{-3}$ with $E_0(\rho) = E(\rho, 0)$ the EOS of SNM, its incompressibility $K_0 \equiv [9\rho^2 \mathrm{d}^2 E_0(\rho)/\mathrm{d}\rho^2]_{\rho_0} = 230\,\mathrm{MeV}$ [22, 23, 24, 25, 26], the isoscalar nucleon k-mass, i.e., $M_0^*(\rho)/M = [1 + (M/|\mathbf{k}|)\mathrm{d}U_0/\mathrm{d}|\mathbf{k}|]^{-1}_{|\mathbf{k}|=k_\mathrm{F}}$, is selected as $M_0^*(\rho_0)/M = 0.58$, and $U_0(\rho_0, 0) = -100\,\mathrm{MeV}$. For the isospin-dependent part in ANM, we adopt $E_\mathrm{sym}(\rho_0) = 31.6\,\mathrm{MeV}$ for the symmetry energy, $L \equiv L(\rho_0) = 58.9\,\mathrm{MeV}$ [27] for the slope of the symmetry energy and $U_\mathrm{sym}(\rho_0, 1\,\mathrm{GeV}) = -20\,\mathrm{MeV}$ [28] for the symmetry potential, respectively. Moreover, the value of Λ is constrained to fall within a reasonable range to guarantee the effect of the high order terms in δ in the EOS of ANM mainly characterized by the fourth order symmetry energy, i.e., $E_\mathrm{sym,4}(\rho) \equiv 24^{-1}\partial^4 E(\rho, \delta)/\partial\delta^4|_{\delta=0}$, is smaller than 3 MeV at ρ_0, to be consistent with predictions of microscopic many-body theories. Consequently, $1.40\,\mathrm{GeV} \lesssim \Lambda \lesssim 1.64\,\mathrm{GeV}$ is obtained and the study based on $\Lambda = 1.6\,\mathrm{GeV}$ is used as the default one. It is worth noting that the single-nucleon potential in SNM thus constructed is consistent with the global relativistic nucleon optical potential extracted from analyzing nucleon-nucleus scattering data [21]. Thus, totally five isoscalar parameters, i.e., $A_\mathrm{t} \equiv A_\ell + A_\mathrm{u}, B, C_\mathrm{t} \equiv C_\ell + C_\mathrm{u}, \sigma$ and a for SNM, and three isovector parameters, i.e., $A_\mathrm{d} \equiv A_\ell - A_\mathrm{u}, C_\mathrm{d} \equiv C_\ell - C_\mathrm{u}$ and x are all fixed. Details values of these parameters for the three cases using the same set of input physical properties are shown in Tab. 1 .

SRC effects on the density dependence of nuclear symmetry energy

Now we turn to effects of the SRC on nuclear symmetry energy. Shown in Fig. 1 are the results obtained using the FFG, HMT-SCGF and HMT-exp parameter sets. By construction, they all have the same $E_\mathrm{sym}(\rho_0)$ and L at ρ_0. Also shown are the constraints on the $E_\mathrm{sym}(\rho)$ around ρ_0 from analyzing intermediate energy heavy-ion collisions (HIC) [29] and the isobaric analog states (IAS) [30]. Although the predicted $E_\mathrm{sym}(\rho)$ using the three parameter sets can all pass through these constraints, they behave very differently especially at supra-saturation densities. The uncertainty of the $E_\mathrm{sym}(\rho)$ due to that of the Λ parameter is also shown in Fig. 1 for the HMT-exp set with the gray dash-dot lines. It is seen that the uncertainty is much smaller than the SRC effect. For example, the variation of the symmetry energy at $3\rho_0$ owing to the uncertainty of Λ is about 2.3 MeV while the SRC effect is about 14.5 MeV. Since the Λ parameter mainly affects the high density/momentum behavior of the EOS, its effects become smaller at lower densities. The reduction of the $E_\mathrm{sym}(\rho)$ at both sub-saturation and supra-saturation densities leads to a reduction of the curvature coefficient $K_\mathrm{sym} \equiv 9\rho_0^2 \mathrm{d}^2 E_\mathrm{sym}(\rho)/\mathrm{d}\rho^2|_{\rho=\rho_0}$ of the symmetry energy. More quantitatively, we find that the K_sym changes from −109 MeV in the FFG set to about −121 MeV and −188 MeV in the HMT-SCGF and HMT-exp set,

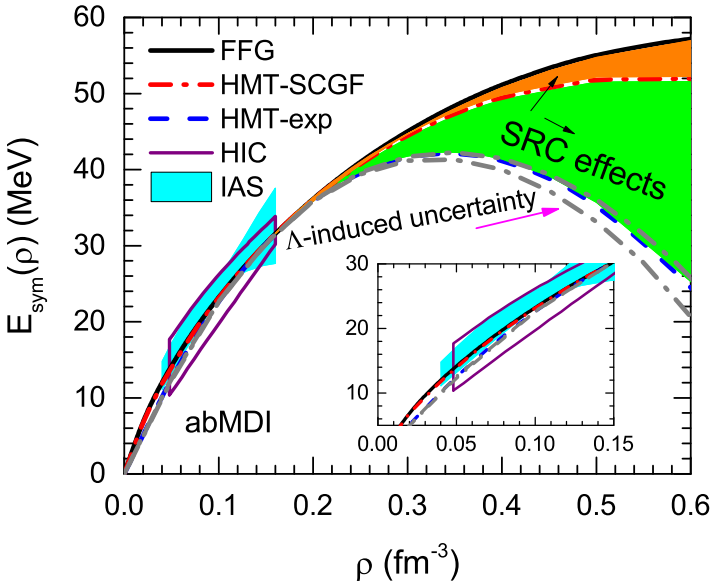

FIGURE 1. Density dependence of nuclear symmetry energy $E_{\rm sym}(\rho)$ using the FFG, HMT-SCGF and HMT-exp parameter set, respectively. Constraints on the symmetry energy from analyzing heavy-ion collisions (HIC) [29] and isobaric analog states (IAS) [30] are also shown for comparisons. The uncertainty range due to the Λ parameter is indicated with the gray dash-dot lines for the HMT-exp set. Taken from refs. [11, 20].

respectively. It is interesting to stress that this SRC reduction of $K_{\rm sym}$ help reproduce the experimentally measured isospin-dependence of incompressibility $K(\delta) = K_0 + K_\tau\delta^2 + O(\delta^4)$ in ANM where $K_\tau = K_{\rm sym} - 6L - J_0L/K_0$. The skewness of SNM $J_0 \equiv 27\rho_0^3 {\rm d}^3E_0(\rho)/{\rm d}\rho^3|_{\rho=\rho_0}$ is approximately −381, −376 and −329 MeV in the FFG, HMT-SCGF and HMT-exp set, respectively. The resulting K_τ is found to change from −365 MeV in the FFG set to about −378 MeV and −457 MeV in the HMT-SCGF and HMT-exp set, respectively. The latter is in good agreement with the best estimate of $K_\tau \approx -550 \pm 100$ MeV from analyzing several different kinds of experimental data currently available [26].

It is also interesting to notice that the SRC-induced reduction of $E_{\rm sym}(\rho)$ within the non-relativistic EDF approach here is qualitatively consistent with the earlier finding within the nonlinear Relativistic Mean-Field (RMF) theory [9]. Nevertheless, since there is no explicit momentum dependence in the RMF EDF, the corresponding reduction of $E_{\rm sym}(\rho)$ is smaller. Obviously, the momentum-dependent interaction makes the softening of the symmetry energy at supra-saturation densities more evident. This naturally leads us to the question why the SRC reduces the $E_{\rm sym}(\rho)$ at both sub-saturation and supra-saturation densities. The SRC affects the $E_{\rm sym}(\rho)$ through several terms. First of all, because of the momentum-squared weighting in calculating the average nucleon kinetic energy, the isospin dependence of the HMT makes the kinetic symmetry energy different from the FFG prediction as already pointed out in several earlier studies [31, 32, 33, 34, 35, 36, 37]. More specifically, within the parabolic approximation of ANM's EOS the $E_{\rm sym}(\rho)$ is approximately the energy difference between PNM and SNM. Thus, the larger HMT due to the stronger SRC dominated by the neutron-proton isosinglet interaction increases significantly the average energy per nucleon in SNM but has little effect on that in PNM, leading to a reduction of the kinetic symmetry energy.

It is worth emphasizing that we focused on effects of the SRC on the symmetry energy of uniform and cold neutron-rich nucleonic matter within the quasi-nucleon picture. It is known that at very low densities symmetric nuclear matter is unstable against forming clusters, such as deuterons and alphas. For studies on the symmetry free energy of clustered matter at finite temperature we refer the readers to refs. [38, 39].

In summary, within a modified non-relativistic GHF-EDF approach and using a new momentum regulating function, we studied effects of SRC-induced HMT in the single-nucleon momentum distribution on the density dependence of nuclear symmetry energy. After re-optimizing the modified GHF-EDF by reproducing the same empirical properties of ANM, SNM and major features of nucleon optical potential at saturation density, the $E_{\rm sym}(\rho)$ was found to decrease at both sub-saturation and supra-saturation densities, leading to a reduced curvature

$K_{\rm sym}$ of $E_{\rm sym}(\rho)$ and subsequently a smaller K_τ for the isospin-dependence of nuclear incompressibility in better agreement with its experimental value. Moreover, the SRC-modified EOS and the single-nucleon potentials in ANM can be used in future transport model simulations of heavy-ion collisions to investigate SRC effects in dense neutron-rich matter in terrestrial laboratories.

Acknowledgement

We thank X.H. Li, W.J. Guo and X.T. He for helpful discussions in earlier studies on this topic. This work was supported in part by the U.S. Department of Energy, Office of Science, under Award Number DE-SC0013702, the CUSTIPEN (China-U.S. Theory Institute for Physics with Exotic Nuclei) under the US Department of Energy Grant No. DE-SC0009971 and the National Natural Science Foundation of China under Grant No. 11320101004 and 11625521, the Major State Basic Research Development Program (973 Program) in China under Contract No. 2015CB856904, the Program for Professor of Special Appointment (Eastern Scholar) at Shanghai Institutions of Higher Learning, Key Laboratory for Particle Physics, Astrophysics and Cosmology, Ministry of Education, China, and the Science and Technology Commission of Shanghai Municipality (11DZ2260700).

REFERENCES

[1] H.A. Bethe, Ann. Rev. Nucl. Part. Sci. **21**, 93 (1971).
[2] A.N. Antonov, P.E. Hodgson, and I.Zh. Petkov, Nucleon Momentum and Density Distribution in Nuclei, Clarendon Press, Oxford, 1988.
[3] J. Arrington, D.W. Higinbotham, G. Rosner, and M. Sargsian, Prog. Part. Nucl. Phys. **67**, 898 (2012).
[4] C. Ciofi degli Atti, Phys. Rep. **590**, 1 (2015).
[5] O. Hen, G.A. Miller, E. Piasetzky, and L.B. Weistein, Review of Modern Physics **89**, 045002 (2017).
[6] A. Rios, A. Polls, and W.H. Dickhoff, Phys. Rev. C **79**, 064308 (2009); *ibid* C **89**, 044303 (2014).
[7] B.J. Cai and B.A. Li, Phys. Rev. C **92**, 011601(R) (2015).
[8] B.J. Cai and B.A. Li, Phys. Lett. **B759**, 79 (2016).
[9] B.J. Cai and B.A. Li, Phys. Rev. C **93**, 014619 (2016).
[10] B.J. Cai, B.A. Li, and L.W. Chen, Phys. Rev. C **94**, 061302(R) (2016)
[11] B.A Li, B.J. Cai, L.W. Chen and J. Xu, Progress in Particle and Nuclear Physics **99**, 29 (2018).
[12] J. Decharge and D. Gogny, Phys. Rev. C **21**, 1568 (1980).
[13] C. Gale, G. Bertsch, and S. Das Gupta, Phys. Rev. C **35**, 1666 (1987).
[14] C.B. Das, S. Das Gupta, C. Gale, and B.A. Li, Phys. Rev. C **67** (2003) 034611
[15] L.W. Chen, C.M. Ko, and B.A. Li, Phys. Rev. Lett.**94**, 032701 (2005).
[16] L.W. Chen, C.M. Ko, B.A. Li, C. Xu, and J. Xu, Eur. Phys. J. A **50**, 29 (2014).
[17] G. F. Bertsch and S. Das Gupta, Phys. Rep. **160**, 189 (1988).
[18] J. Aichelin, Phys. Rep. **202**, 233 (1991).
[19] B.A. Li, L.W. Chen, and C.M. Ko, Phys. Rep. **464**, 113 (2008).
[20] B.J. Cai and B.A. Li, arXiv:1703.08743.
[21] S. Hama, B.C. Clark, E.D. Cooper, H.S. Sherif, and R.L. Mercer, Phys. Rev. C **41**, 2737 (1990).
[22] D.H. Youngblood, H.L. Clark, and Y.-W. Lui, Phys. Rev. Lett. **82**, 691 (1999).
[23] S. Shlomo, V.M. Kolomietz, and G Colò, Eur. Phys. J. A **30**, 23 (2006).
[24] J. Piekarewicz, J. Phys. G **37**, 064038 (2010).
[25] L.W. Chen and J.Z. Gu, J. Phys. G **39**, 035104 (2012).
[26] G. Colò, U. Garg and H. Sagawa, Eur. Phys. J. A **50**, 26 (2014).
[27] B.A. Li and X. Han, Phys. Lett. **B727**, 276 (2013).
[28] J. Xu, L.W. Chen, and B.A. Li, Phys. Rev. C **91**, 014611 (2015).
[29] B.M. Tsang *et al.*, Phys. Rev. C **86**, 105803 (2012).
[30] P. Danielewicz and J. Lee, Nucl. Phys. **A922**, 1 (2014).
[31] C. Xu and B.A. Li, arXiv:1104.2075.
[32] C. Xu, A. Li, B.A. Li, J. of Phys: Conference Series **420**, 012190 (2013).
[33] O. Hen, B.A. Li, W.J. Guo, L.B. Weinstein, and E. Piasetzky, Phys. Rev. C **91**, 025803 (2015).
[34] I. Vidaña, A. Polls, and C. Providência, Phys. Rev. C **84**, 062801(R) (2011).
[35] A. Lovato, O. Benhar, S. Fantoni, A.Yu. Illarionov, and K.E. Schmidt, Phys. Rev. C **83**, 054003 (2011).
[36] A. Carbone, A. Polls, A. Rios, Eur. Phys. Lett. **97**, 22001 (2012).
[37] A. Carbone, A. Polls, C. Providência, A. Rios, and I. Vidaña, Eur. Phys. A **50**, 13 (2014).
[38] J.B. Natowitz et al, Phys. Rev. Lett. **104**, 202501 (2010).
[39] S. Type, H. Wolter H, G. Röpke and D. Blaschke, Euro Phys J A **50**, 17 (2014).